

# Three-axis Laser Method for Measuring the Diameter of Cylindrical Objects

E.M. Fedorov<sup>1</sup>, A.A. Koba

National Research Tomsk Polytechnic University  
Tomsk, Russia

<sup>1</sup> E-mail: evgeny\_fyodorov@list.ru

**Abstract**—The paper presents a three-axis method for measuring the diameter and ovality of cylindrical objects in the divergent laser beam. The mathematical expressions to calculate the diameter using measuring devices based on this method have been obtained. The research results can be used to develop and manufacture noncontact optical devices for in-process control of the outer diameter of products in cable, pipe and other industries.

**Keywords**—component; three-axis method, in-process diameter measurement, divergent beam, multi-element receivers, diameter calculation.

## I. INTRODUCTION

Various geometric and electrical parameters are used to assess the quality of cable products. The rejects can be minimized through the improved technology to control the product major characteristics, namely capacitance per unit length [1, 2], eccentricity [3], outer diameter [4-6], insulation integrity [7] and others parameters [8-12].

Noncontact gauges for measuring the diameter of circular long-length objects such as cables, ropes, pipes, etc., which are based on the shadow measuring method using the divergent luminous flux, exhibit a number of undeniable advantages since they do not use the elements of lens and mirror optics. In particular, the measurement accuracy obtained by these devices using a combination of diffraction methods and statistical data processing may be of micrometer fractions [13,14]. However, when measurement is performed using the divergent light flux, the shadow dimensions of the measured object change in case the object is displaced within the test zone. This requires the use of complex ratios to calculate the true diameter of the object [15]. Two-coordinate measuring gauges provide approximate values of the ovality estimated on the basis of the difference between the diameters of the two measuring axes, which are directly dependent on the object orientation within the measuring field. In this case, particular positions of the object do not allow the ovality fixation. Fig. 1 shows an example of this orientation for an object with an ellipsoidal cross-section. The cross-section images  $D_x$  and  $D_y$  in the multi-element receivers of measuring channels  $X$  and  $Y$  are equal and they cannot provide the ovality parameters.

The measurements performed in the three-axis laser systems with a divergent laser beam can partially solve the above-stated problems. Three-axis measuring gauges exhibit

the following advantages when compared with those of two-axis devices: three synchronized measuring axes on the same plane; detection of any deviation from the circular cross-section regardless of the object orientation in the measured zone; determination of the circumference and area of the cross-section.

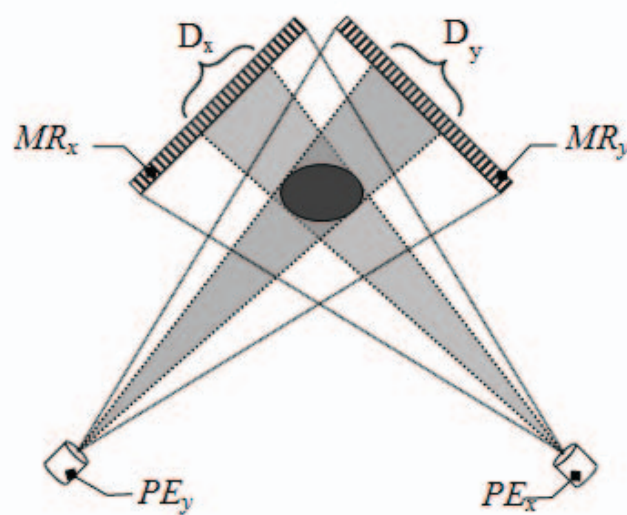


Fig. 1. Example of orientation of the object with a non-circular cross-section, in which the calculation of ovality parameters is impossible.  $MR_x$ ,  $PE_x$  and  $MR_y$ ,  $PE_y$  are multi-element receivers and point emitters of measuring axes  $Y$  and  $X$ , respectively.  $D_x$  and  $D_y$  are images of the object shadows in the corresponding photoreceivers.

## II. DIAMETER CALCULATION

Since the true diameter is a calculated value in both three- and two-axis laser systems, the derivation of mathematical expressions for its calculation is required.

Fig. 2 shows the schematic diagram of the considered three-axis measuring gauge. The device comprises three measuring channels, with  $X$ ,  $Y$  and  $Z$  axes arranged at  $120^\circ$  angle to each other. Each channel has a point emitter (semiconductor laser) generating a divergent luminous flux and a multi-element photoreceiver measuring the size of the shadow falling on the object. The measuring object is found in the test zone; it is illuminated by three emitters and form three shadows in photoreceiver of the corresponding measuring channels.

The known design parameters of the device are as follows:

Distances  $H_x$ ,  $H_y$  and  $H_z$  from the emitter center to the plane of the receiver of each channel:  $(S_{X0}; B_{X0})$ ,  $(S_{Y0}; B_{Y0})$  and  $(S_{Z0}; B_{Z0})$  segments.

Distances  $H_{X0}$ ,  $H_{Y0}$  and  $H_{Z0}$  from the center of the emitter to the center of the test zone, i.e. the point  $(O)$ , which is an imaginary point for intersection of the measuring channel symmetry axes.

The step of the photoreceiver cells allows measurement of the shadow, i.e. its width, in the number of cells shadowed by the object, and the displacement of the shadow center relative to the "zero" cell of the receiver.

The known data are used to measure the object radii by the three channels  $(R_x, R_y, R_z)$  and to determine the average radius  $R_{av}$  and the object ovality. To perform special measurements, data on the object position is required, (displacement of its  $Z$  center) relative to the center of the gauge test zone (" $O$ " point), i.e. the  $E_x$ ,  $E_y$  and  $E_z$  values.

The problem is solved in three steps:

Step 1 – determination of the position of the  $Z$  object center projection in the plane of the "X", "Y" and "Z" receivers.

The position of the center projection is characterized by the  $X_0$ ,  $Y_0$  and  $Z_0$  values, which are  $(B_{X0}; X_0)$ ,  $(B_{Y0}; Y_0)$  and  $(B_{Z0}; Z_0)$  segments. According to the triangle  $(S_{X0}; B_{X0}; X_0)$ , it is known that:

$$\operatorname{tg}(\alpha + \alpha_1) = \frac{X_0}{H_x}. \text{ Hence: } X_0 = H_x \cdot \operatorname{tg}(\alpha + \alpha_1) \quad (1)$$

The value  $\alpha_1$  in expression (1) can be found through the triangle  $(S_{X0}; B_{X0}; X_1)$ :

$$\operatorname{tg}\alpha_1 = \frac{X_1}{H_x}; \alpha_1 = \operatorname{arctg} \frac{X_1}{H_x}. \quad (2)$$

The angle  $\alpha$  is determined through the triangle  $(S_{X0}; B_{X0}; X_2)$ :

$$\operatorname{tg}(\alpha + \alpha + \alpha_1) = \frac{X_2}{H_x}; (2\alpha + \alpha_1) = \operatorname{arctg} \frac{X_2}{H_x}.$$

With regard to expression (2), the ratio of the angle  $\alpha$  takes the form:

$$\alpha = \frac{1}{2}(\operatorname{arctg} \frac{X_2}{H_x} - \operatorname{arctg} \frac{X_1}{H_x}) \quad (3)$$

Substitution of (3) and (2) in (1) and transformations result in:

$$X_0 = H_x \cdot \operatorname{tg} \frac{1}{2}(\operatorname{arctg} \frac{X_2}{H_x} + \operatorname{arctg} \frac{X_1}{H_x}) \quad (4)$$

The same procedure is performed for  $Y_0$  and  $Z_0$  values:

$$Y_0 = H_y \cdot \operatorname{tg} \frac{1}{2}(\operatorname{arctg} \frac{Y_2}{H_y} + \operatorname{arctg} \frac{Y_1}{H_y}) \quad (5)$$

$$Z_0 = H_z \cdot \operatorname{tg} \frac{1}{2}(\operatorname{arctg} \frac{Z_2}{H_z} + \operatorname{arctg} \frac{Z_1}{H_z}) \quad (6)$$

Similarity of the triangles  $(S_{X0}; B_{X0}; X_0)$  and  $(S_{X0}; O_x; Z)$  provides:

Step 2 – determination of the  $Z$  object center displacement relative to the center of the test zone. The displacement is characterized by  $E_x$ ,  $E_y$  and  $E_z$  values (Fig. 1).

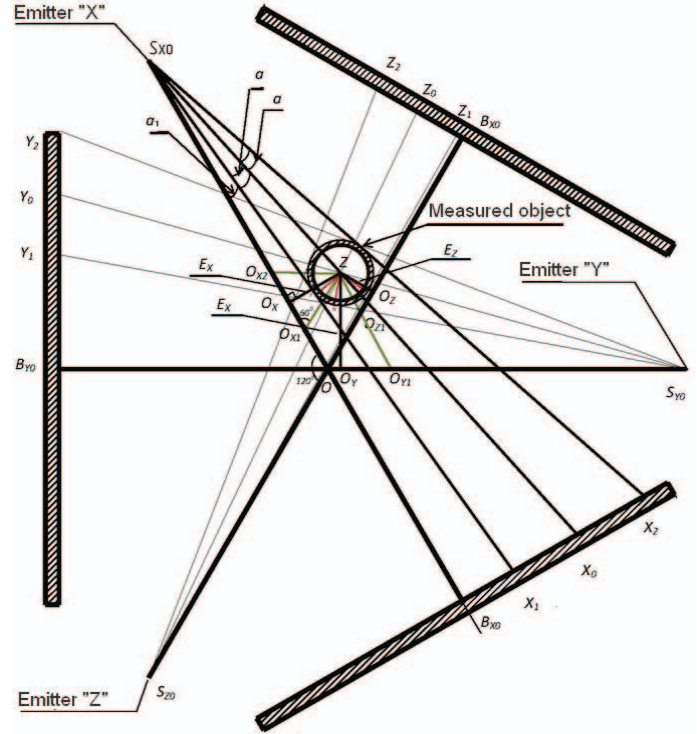


Fig. 2. Calculation model for the device with three measuring axes.

$$\frac{E_x}{X_0} = \frac{(S_{X0}; O_x)}{H_x}. \text{ Similarly: } \frac{E_y}{Y_0} = \frac{(S_{Y0}; O_y)}{H_y}; \quad (7)$$

$$\frac{E_z}{Z_0} = \frac{(S_{Z0}; O_z)}{H_z}$$

Find the values for the segments  $(S_{X0}; O_x)$ ,  $(S_{Y0}; O_y)$  and  $(S_{Z0}; O_z)$  in (7), provided the segment  $(O; O_x)$  is:

$$(O; O_x) = (Z; O_{Y1}) - (O_{X2}; O_x) = \frac{E_y}{\cos(\frac{\pi}{6})} - \frac{E_x}{\operatorname{tg}(\frac{\pi}{3})};$$

$$\text{segment } (O; O_y) = (Z; O_{X2}) - (O_y; O_{Y1}) = \frac{E_x}{\cos(\frac{\pi}{6})} - \frac{E_y}{\operatorname{tg}(\frac{\pi}{3})}.$$

$$\text{segment } (O; O_z) = (Z; O_{X1}) + (O_z; O_{Z1}) = \frac{E_x}{\cos(\frac{\pi}{6})} + \frac{E_z}{\operatorname{tg}(\frac{\pi}{3})}.$$

Then:

$$\begin{aligned}(S_{X0}; 0_X) &= H_{X0} - \frac{E_Y}{\cos(\frac{\pi}{6})} + \frac{E_X}{\operatorname{tg}(\frac{\pi}{3})} \\(S_{Y0}; 0_Y) &= H_{Y0} - \frac{E_X}{\cos(\frac{\pi}{6})} + \frac{E_Y}{\operatorname{tg}(\frac{\pi}{3})}; \\(S_{Z0}; 0_Z) &= H_{Z0} + \frac{E_X}{\cos(\frac{\pi}{6})} + \frac{E_Z}{\operatorname{tg}(\frac{\pi}{3})}\end{aligned}\quad (8)$$

With regard to expression (8), ratios (7) take the form:

$$\begin{aligned}\frac{E_X}{X_0} &= \frac{H_{X0} - \frac{E_Y}{\cos(\frac{\pi}{6})} + \frac{E_X}{\operatorname{tg}(\frac{\pi}{3})}}{H_X}; \\ \frac{E_Y}{Y_0} &= \frac{H_{Y0} - \frac{E_X}{\cos(\frac{\pi}{6})} + \frac{E_Y}{\operatorname{tg}(\frac{\pi}{3})}}{H_Y}; \\ \frac{E_Z}{Z_0} &= \frac{H_{Z0} + \frac{E_X}{\cos(\frac{\pi}{6})} + \frac{E_Z}{\operatorname{tg}(\frac{\pi}{3})}}{H_Z}\end{aligned}\quad (9)$$

Expressions (9) are a system of three equations with three unknowns:  $E_X$ ,  $E_Y$  and  $E_Z$ . Solve the equations and derive the expressions to calculate  $E_X$ ,  $E_Y$  and  $E_Z$ , in which the  $X_0$ ,  $Y_0$  and  $Z_0$  values are calculated by (4), (5) and (6) ratios. This paper does not provide the extended expressions for calculation of the system of equations in letter values.

Step 3 – calculation of the object radii  $R_X$ ,  $R_Y$  and  $R_Z$ .

The schematic diagram in Figure 1 indicates that the  $R_X$  radius, i.e. the segment ( $F;Z$ ), is the side of the right triangle ( $S_{X0}; Z; F$ ). According to this triangle:

$$R_X = (S_{X0}; Z) \cdot \sin \alpha \quad (10)$$

The other right triangle ( $S_{X0}; Z; 0_X$ ) is used to find the segment ( $S_{X0}; Z$ ):

$$\begin{aligned}(S_{X0}, Z) &= \sqrt{(0_X; Z)^2 + (0_X; S_{X0})^2} = \\ &= \sqrt{E_X^2 + (H_{X0} - \frac{E_Y}{\cos(\frac{\pi}{6})} + \frac{E_X}{\operatorname{tg}(\frac{\pi}{3})})^2}.\end{aligned}$$

Substitute the value of the segment ( $S_{X0}; Z$ ) in (10) and use expression (3) for the angle  $\alpha$  to find the radius  $R_X$ .

$$\begin{aligned}R_X &= \sqrt{E_X^2 + (H_{X0} - \frac{E_Y}{\cos(\frac{\pi}{6})} + \frac{E_X}{\operatorname{tg}(\frac{\pi}{3})})^2} \cdot \\ &\cdot \sin \frac{1}{2} (\operatorname{arctg} \frac{X_2}{H_X} - \operatorname{arctg} \frac{X_1}{H_X})\end{aligned}\quad (11)$$

Similarly:

$$\begin{aligned}R_Y &= \sqrt{E_Y^2 + (H_{Y0} - \frac{E_X}{\cos(\frac{\pi}{6})} + \frac{E_Y}{\operatorname{tg}(\frac{\pi}{3})})^2} \cdot \\ &\cdot \sin \frac{1}{2} (\operatorname{arctg} \frac{Y_2}{H_Y} - \operatorname{arctg} \frac{Y_1}{H_Y})\end{aligned}\quad (12)$$

$$\begin{aligned}R_Z &= \sqrt{E_Z^2 + (H_{Z0} + \frac{E_X}{\cos(\frac{\pi}{6})} + \frac{E_Z}{\operatorname{tg}(\frac{\pi}{3})})^2} \cdot \\ &\cdot \sin \frac{1}{2} (\operatorname{arctg} \frac{Z_2}{H_Z} - \operatorname{arctg} \frac{Z_1}{H_Z})\end{aligned}\quad (13)$$

The values of the  $R_X$  and  $R_Y$  radii being known, the average radius  $R_{av}$  of the object and object ovality ( $O$ ) can be found.

$$R_{av} = \frac{|R_X| + |R_Y| + |R_Z|}{3}; \quad O = (R_{\max} - R_{\min}) \quad (14)$$

### III. METHOD EVALUATION

A three-axis optical device for measuring the diameter of cylindrical objects has been simulated to verify the above suggested expressions (11–13). A computer model presented in Fig. 2 comprises three identical measuring channels arranged at  $120^\circ$  to each other. The initial geometric parameters to simplify calculations are the same for all the measuring channels:

- The distance from the emitter center to the plane of the receiver  $H_x=H_y=H_z=300$  (mm).
- The distance from the emitter center to the test zone, i.e. the center of intersection of the measuring channel axes  $H_{X0}=H_{Y0}=H_{Z0}=220$  (mm).

Such values of the optical devices geometric parameters are typical for the measurement area sufficient for most applications. In this model, the length of the working surface of multiple-receiver does not exceed 100 mm. All the initial geometrical parameters and virtual positions of shadows in the radiation receiver planes in the corresponding channels (Fig. 2)  $X_1, X_2, Y_1, Y_2, Z_1$  and  $Z_2$ , were determined in the computer model with 1  $\mu\text{m}$  error. Round objects with different diameters and different location in the virtual measuring zone were simulated to perform testing. When substituting the values obtained during the simulation into expressions (11–13), the measuring object diameters were calculated in the corresponding measuring axes  $X$ ,  $Y$  and  $Z$ . These calculated diameters  $D_x, D_y, D_z$  for three arbitrary circular objects with the diameter  $D$  are presented in Table 1.

TABLE I.

Diameter values and the error for three axes							
Measuring diameter $D$ (mm)	Diameter $D_x$ (mm)	Error $\Delta D_x$ ( $\mu\text{m}$ )	Diameter $D_y$ (mm)	Error $\Delta D_y$ ( $\mu\text{m}$ )	Diameter $D_z$ (mm)	Error $\Delta D_z$ ( $\mu\text{m}$ )	Error $\Delta D_{av}$ ( $\mu\text{m}$ )
10.000	10.003	-3	10.002	-2	9.998	2	-1
17.000	16.997	3	16.999	1	17.002	-2	0.67
25.000	24.999	1	25.001	-1	25.000	0	0

The absolute error of the diameter calculation in the measuring axes  $\Delta D_x$ ,  $\Delta D_y$  and  $\Delta D_z$ , as well as the mean error  $\Delta D_{av}$  do not exceed 3  $\mu\text{m}$ , that is acceptable with regard to the error in the initial parameter determination. In practice, the diameter calculation accuracy strongly depends on the accuracy of initial parameters. The mechanisms to solve the above-stated problem are considered in [16,17]. Further simulation of the three-axis device is to be performed on a real prototype using the methods of digital signal processing. Due to this, the error in the diameter calculation may be of micrometer fractions.

#### IV. CONCLUSION

This paper proposes a method for three-axis measurement of the diameter using a divergent laser beam. Expressions (9, 11–14) have been derived to calculate the precise value of the object radii, the coordinates of the object center position, and the average radius and the precise value of its ovality in the maximum and minimum values. Realized computer simulation three-axis transducer, which confirmed the correctness of the proposed conversion function. The described optical method and mathematical support can be used to design a primary measuring transducer for the device to test the diameter and ovality of long-length products.

#### ACKNOWLEDGMENTS

The authors gratefully acknowledge the great assistance of Y. A. Chursin and translation by M. A. Yuzhakova from Tomsk Polytechnic University

#### REFERENCES

[1] N.S. Starikova., V.V. Redko. and G.V. Vavilova, "Control of Cable Insulation Quality by Changing of Electrical Capacitance Per Unit During," High Voltage Testing Journal of Physics: Conference Series 671 012056.

[2] A.E. Goldshtein., G.V. Vavilova. and V.Yu. Belyankov, "An electro-capacitive measuring transducer for the process inspection of the cable

capacitance per unit length in the process of production," Russian Journal of Nondestructive Testing, Vol. 51, No. 2, 2015, pp. 35–43.

[3] A.E. Goldshtein. and E.M. Fedorov, "A Mutually Inductive Measuring Transducer of Transverse Displacements of a Rectilinear Conductor," Russian journal of nondestructive testing, Vol. 46.

[4] E.M. Fedorov., A.E. Goldshtein., V.V. Red'ko, "Methods and instruments for the optical control of the diameter and ovality of electrical cables during manufacturing," Polzunovsky Vestnik, 2010, No. 2.

[5] E.M. Fedorov., I. Bortnikov, "Monitoring of the outer diameter of long items using the optical diffraction method," Technical Physics, Vol. 60, Issue 11, pp. 1689–1692.

[6] S. A. Khodier, "Measurement of wire diameter by optical diffraction," Opt Laser Technol 2004;36(1):63–7 (Original Research Article)

[7] V.V. Red'ko., A.P. Leonov., L.A. Red'ko., V.A. Bolgova, "Problems of Automatic Test of Insulation in Cable Production," Journal of Physics: Conference Series, Vol. 671.

[8] I. V. Plotnikova, O. N. Chaykovskaya, A. Yu. Petrova, "Investigation of bactericide systems using a microfiber polypropylene carrier," Technical Physics : Scientific Journal, vol. 60, iss. 4, 2015, pp. 592-594.

[9] R. M. Mustafina, I. A. Plotnikov, I. V. Plotnikova, O. N. Tchaikovskaya, "Choice of Parameters and Stability of Nonlinear Vibration Isolation Device," Journal of Physics: Conference Series, 2016, vol. 671, 012046, pp. 1-5.

[10] V. N. Borikov, O. V. Galtseva, G. A. Filippov, "Method of Noncontact Calibration of the Robotic Ultrasonic Tomograph," Journal of Physics: Conference Series, 2016, vol. 671, 012014, pp. 1-7.

[11] A.P. Surzhikov., T.S. Frangulyan., S.A. Ghyngazov., E.N. Lisenko., O.V. Galtseva, "Physics of magnetic phenomena: Investigation of electroconductivity of lithium pentaferriite," Russian Physics Journal, vol. 49 (5), 2006, pp. 506-510.

[12] A.P. Surzhikov, T.S. Frangulyan, S.A. Ghyngazov E.N. Lysenko, "Investigation of structural states and oxidation processes in Li 0.5Fe2.5O4- $\delta$  using TG analysis," Journal of Thermal Analysis and Calorimetry Volume 108, Issue 3, June 2012, Pages 1207-1212.

[13] Y.A. Chursin, Evgeny M. Fedorov, "Methods of resolution enhancement of laser diameter measuring instruments," Optics & Laser Technology, Vol. 67, 2015, pp. 86–92.

[14] L. Jinhuan, S. Osami, S. Takamasa, "Measurement of diameter of metal cylinders using a sinusoidally vibrating interference pattern," Opt Commun 2006;260(2):398–402

[15] A.R. Svendrovskii., "Raschet diametra v beskontaktnykh dvukhkoordinatnykh izmeritelyakh," Proceedings of the 1st all-Russian science conference on Scientific and Engineering problems of instrument engineering. Tomsk; 2005, pp. 31–33.

[16] Y. Chugui., V. Bazin., L. Finogenov., S. Makarov., A. Verkhogliad, "Optical electronic measuring systems and laser technologies for scientific and industrial applications," Proceedings of the international symposium on instrumentation and control technology No. 6, Beijing, China. 2006. vol. 6357

[17] E.M. Fedorov., A.A. Edlichko, "Vychislenie geometricheskikh parametrov dvukh-koordinatnykh izmeritelei diametra protyazhennykh izdelii," Bulletin of the Tomsk Polytechnic University, 2008. No. 2. (rus).